Strong Metal–Support Interactions. Group 8 Noble Metals Supported on TiO_2

S. J. Tauster,* S. C. Fung, and R. L. Garten

Contribution from the Exxon Research and Engineering Company, Corporate Research Laboratories, Linden, New Jersey 07036. *Received July 15, 1977*

Abstract: The reduction of noble metals supported on TiO_2 at low temperatures (200 °C) produces well-dispersed metals which exhibit the capacity to sorb both hydrogen and carbon monoxide. Reduction of the same materials at 500 °C, however, decreases hydrogen and carbon monoxide sorption to near zero in all cases. Electron microscopy and x-ray diffraction show that the loss of this sorption capacity is not due to metal agglomeration. This effect for well-dispersed metals is evidence for a chemical interaction between the noble metal and the support. The nature of the interaction is discussed in terms of metal–metal bonding between the noble metal and titanium cations or, alternatively, the formation of intermetallic compounds.

Introduction

In addition to their technological importance, supported-metal catalysts are of interest due to the unique materials-scientific problems they pose. One of these relates to the degree of interaction that may exist between a small metal crystallite and the underlying surface.

Evidence has been presented in recent years that in certain instances the support can influence the metal phase in ways other than simply pertaining to dispersion. Thus, Dalmai-Imelik et al.[1] reported a "chemoepitaxial effect" on the growth of nickel crystallites during the reduction of nickel antigorite. Depending upon conditions of reduction, either (111) or (110) orientations of nickel emanating from the antigorite structure were obtained. In another study, Dalla Betta and Boudart[2] prepared small clusters of platinum in a Y zeolite and observed anomalously high activities for hydrogenation, isomerization, and hydrogenolysis. The authors proposed electron-deficient platinum clusters, perhaps due to partial electron transfer to the zeolite. Gallezot et al.[3] investigated the Pt–Y zeolite system with IR spectroscopy in combination with benzene hydrogenation and poisoning studies. They observed that hydroxylated and dehydroxylated zeolites behaved similarly and interpreted this to mean that the electron-deficient nature of platinum agglomerates situated in supercages is an intrinsic property of very small particles rather than the result of an interaction with electron-acceptor sites of the zeolite.

The Pt–Y zeolite catalyst described by Dalla Betta and Boudart[2] manifested normal hydrogen-chemisorption properties. Indeed, there does not seem to be any clear evidence yet reported of a support effect related change in the hydrogen-adsorption (or CO-adsorption) properties of group 8 metals. In this regard a study by Gallezot et al.,[4] also involving Pt–Y zeolites, may be mentioned. It was found that a particular thermal activation led, after reduction in hydrogen, to atomically dispersed platinum atoms in sodalite cages. In this situation the Pt atoms did not chemisorb hydrogen. As suggested by the authors, this need not indicate a metal–support interaction. Simple inaccessibility of H_2 (2.89 Å kinetic diameter) to the sodalite cage (2.2 Å aperture) or a need for two platinum atoms to dissociate H_2 might be responsible. Treatment at 300 °C or above leads to migration of these atoms out of the sodalite cages to form agglomerates which manifest normal hydrogen-chemisorption behavior. This migration suggests the absence of strong interaction between the platinum and the zeolite.

Several years ago we decided to approach the problem of metal–suppport interactions from the point of view of the solid state chemistry of transition metal compounds. Although almost all studies of supported-metal catalysts have involved non-transition-metal oxides (Al_2O_3, SiO_2, SiO_2–Al_2O_3, SiO_2–MgO), there were reasons for believing that oxides of transition metals might be more likely to interact with metal atoms at their surface. Of particular interest is the phenomen of metal–metal bonding, in which two or more cations are linked by direct covalent bonds. In contrast to main-group metal oxides, metal–metal bonding plays a significant role in the solid state chemistry of many transition metal oxides, the bonding arising from the overlap of d orbitals of neighboring cations. The size and geometrical arrangement of mutually bonded cations (the "metal clusters") varies. Thus, the dioxides of Mo, W, V, Nb, and Re exhibit a distorted rutile structure in which bonded cation pairs occur,[5] $Zn_2Mo_3O_8$ and its isomorphs contain a triangular Mo_3 cluster,[6] while the Ru_3 cluster in $BaRuO_3$ is linear.[7] In the case of $BaNiO_3$ infinite chains of metal–metal-bonded nickel cations extend through the lattice.[8]

Metal clusters in transition metal oxides almost always consist of like atoms, as in all of the above-cited examples. An exception to this was reported by Dickinson, Katz, and Ward,[9] who showed that a class of oxides, the hexagonal barium titanates, are characterized by heteroatomic metal–metal bonding. The general formula for these oxides is $BaM_{1/3}Ti_{2/3}O_{3-x}$ wherein M is the "donor" cation and $x \neq 0$ corresponds to divalency or trivalency of the latter. Donor cations which stabilize the hexagonal barium titanate structure are those of V, Cr, Mn, Fe, Co, Ru, Rh, Ir, Pt, and Ti(3+). The authors suggest that one of every two titanium "host" cations is metal–metal bonded to a donor ion, with the bonding occurring through the shared face connecting adjacent octahedra of the host cation and donor cation. The bonding molecular orbitals are proposed to arise via the overlap of three t_{2g} orbitals from each of these ions.

It seemed reasonable that titanium cations at a *surface* should have the same capacity for metal–metal bonding. As we were interested in supported-metal catalysts under reducing conditions, the "donor" species would necessarily be either a zerovalent (or slightly ionic) metal atom, or, more probably, aggregates of metal atoms. There did not seem to be any reason to exclude the possibility of bonding interactions between d electrons from such an aggregate and d orbitals centered at titanium cations at the surface. It was therefore decided to explore the possibility of strong interactions between noble metals and supports containing titanium cations.

Soon after commencing this study it became apparent that the chemisorption properties of the noble metals were dramatically altered by interactions with a TiO_2 surface. It was decided accordingly to examine each of the noble metals, supported on TiO_2, for this effect and the results of these studies are reported in this paper.

0002-7863/78/1500-0170$01.00/0

Table I. Physical Properties of TiO_2 Supports

Property	TiO_2 (P-25)	TiO_2 (Cab-O-Ti)
Purity, %	>97[a]	99.8
Surface area, $m^2\ g^{-1}$	50 ± 15	50–70
Average particle size, μm	0.03	0.03
Crystal modification	~80% anatase	85% anatase
	~20% rutile	15% rutile

[a] The major impurities reported by the manufacturer are Al_2O_3 <0.3%, HCl <0.3%, SiO_2 <0.2%, SO_3 <0.2%, MgO <0.08%, Na_2O <0.05%, CaO trace, <5 ppm heavy metals.

Experimental Section

Materials. The TiO_2 supports used in this study were obtained from two sources: TiO_2 (P-25) from the Degussa Co. and TiO_2 (Cab-O-Ti) from Cabot Corp. The physical properties of these materials as reported by the manufacturers are summarized in Table I. Both of these materials are prepared by the flame hydrolysis of $TiCl_4$ and their physical properties, as summarized in Table I, are seen to be very similar, the primary difference being the higher purity listed for Cab-O-Ti TiO_2.

The catalysts were prepared by impregnating TiO_2 with metal salt solutions of the appropriate concentrations in a ratio of 0.25 cm^3 per gram of TiO_2. The solutions were added to the TiO_2 in increments of a few drops with thorough mixing between additions. The impregnates were dried in air at 110–120 °C for 16 h. The metal salt solutions were prepared from $H_2OsCl_6{\cdot}6H_2O$, $H_2PtCl_6{\cdot}6H_2O$, $H_2IrCl_6{\cdot}6H_2O$, $RuCl_3{\cdot}3H_2O$, $RhCl_3{\cdot}3H_2O$, and $PdCl_2$. The first five salts were dissolved in distilled water whereas $PdCl_2$ was dissolved in concentrated HCl followed by evaporation to near dryness twice and diluted with distilled water after each evaporation. $H_2OsCl_6{\cdot}6H_2O$ and $RhCl_3{\cdot}3H_2O$ were obtained from Alfa Inorganics, Inc., Beverly, Mass., and the other salts were obtained from Engelhard Industries, Inc., Newark, N.J.

Apparatus and Procedure. Dihydrogen and carbon monoxide sorption studies were performed with a conventional glass vacuum system. The system incorporated an 80-L oil diffusion pump backed by a mechanical pump with liquid nitrogen traps on the inlet and outlet of the diffusion pump. Ultimate dynamic vacua of about 10^{-7} Torr were obtainable. Pressure measurements during sorption studies were made with a Texas Instruments Precision Pressure gauge. Samples of about 1 g and sieved to 20–40 mesh size were placed in flow-through cells made of Vycor.

Samples were reduced in hydrogen in situ at a space velocity of 500 min^{-1}. Reductions were carried out in two temperature regimes. The *high-temperature reduction* (HTR) consisted of H_2 treatment for 1 h at 500 °C, cooling in flowing H_2 to 450 °C, and evacuation at this temperature for 0.5 h. The sample was then cooled under dynamic vacuum to room temperature. Longer evacuation times did not affect the chemisorption results. The *low-temperature reduction* (LTR) consisted of H_2 treatment for 2 h at 200 °C and evacuation for 2 h followed by cooling under dynamic vacuum to room temperature. The only exception to this was the low-temperature treatment for Pd/TiO_2, which consisted of a 1-h reduction and evacuation each at 175 °C.

Dihydrogen and carbon monoxide uptakes were determined at 25 ± 2 °C on the reduced and evacuated samples. Typically, 30–60 min were allowed for each uptake point. The H/M ratios were calculated by assuming that H_2 uptakes at zero pressure of H_2 corresponded to saturation coverage of the metal. These uptakes were determined by extrapolation of the high-pressure linear portion of the isotherm as described by Benson and Boudart[10] and Wilson and Hall.[11] The CO/M ratios were calculated by determining the CO uptakes on the reduced and evacuated samples and assuming that this represented the sum of CO weakly bound to the support and strongly bound to the metal. The sample was then evacuated for 1 min at room temperature and a second CO isotherm measured. Since the second isotherm measures only the CO weakly adsorbed on the support, subtraction of the two isotherms gives the amount of strongly bound CO which is associated with the metal. In accordance with previous studies,[12] the amount of strongly bound CO at 10-cm pressure was chosen as saturation coverage of the metal.

BET surface area measurements were determined with argon at liquid nitrogen temperature. A value of 1.46 nm^2 was assumed for the area of an argon atom and a value of 21 cm was used for P_0.

Table II. Hydrogen and CO Sorption at 25 ± 2 °C on TiO_2-Supported Metals

Metal	Redn temp, °C	H/M	CO/M	BET area, $m^2\ g^{-1}$
2% Ru	200	0.23	0.64	45
	500	0.06	0.11	46
2% Rh	200	0.71	1.15	48
	500	0.01	0.02	43
2% Pd	175	0.93	0.53	42
	500	0.05	0.02	46
2% Os	200	0.21		
	500	0.11		
2% Ir	200	1.60	1.19	48
	500	0.00	0.0	45
2% Pt	200	0.88	0.65	
	500	0.00	0.03	
Blank TiO_2	150[a]	*b*		51
Support	500	*b*		43

[a] Evacuated for 2 h at 150 °C; no reduction prior to BET area determination. [b] H_2 uptake on these samples exhibited Henry's law behavior and was zero at $P_{H_2} = 0$ by extrapolation.

Dihydrogen of 99.95% purity was passed through a Deoxo unit (Englehard Industries, Inc.), a 5A molecular sieve drying trap, an Oxy-trap (Alltech Associates, Arlington Heights, Ill.) to remove last traces of oxygen, and finally a liquid nitrogen trap before being admitted to the catalyst for reductions or chemisorption measurements. Carbon monoxide of 99.99% purity was passed through a dry ice–2-propanol trap before exposure to the sample. Argon of 99.9995% purity was used as received.

A Phillips Electronics x-ray diffractometer (XRG-3000) with nickel-filtered Cu K radiation was used for x-ray diffraction studies of the samples. Particle sizes, where evaluated by x-ray line broadening, were calculated as described elsewhere.[13] Electron microscopy studies were performed on a Phillips EM300 transmission electron microscope described by Prestridge and Yates.[14]

Results

H_2 and CO Sorption. The results of the H_2 and CO sorption studies are summarized in Table II along with the BET surface areas of the samples. Figures 1 and 2 show representative isotherms. Following LTR the H_2 and CO uptakes on all samples are appreciable and correspond to moderate to high dispersions of the metal components. It is possible that the pretreatment conditions for the low-temperature reductions were not optimal for complete reduction and outgassing of all samples. In such case the H/M and CO/M ratios in Table I would represent lower limits on the dispersions of the samples. The H/M and CO/M ratios in excess of unity for Ir/TiO_2 and Rh/TiO_2 are confirmed by repeated experiments. In our laboratories we have frequently observed H/M and CO/M values in excess of unity for Ir/Al_2O_3 and Ir/SiO_2 samples. Engels et al.[15] have also reported H/M ratios of ~2 when Ir was added to Pt/Al_2O_3 samples. Such observations are usually attributed to hydrogen spillover[15] or to multiple bonding of the adsorbate on the corner and edge atoms of very small metal crystallites.[16,17] The important point for our later discussion is not the absolute values of the H/M and CO/M ratios but rather that following low-temperature reductions the noble metal/TiO_2 samples exhibit "normal" chemisorption properties indicative of moderate to high metal dispersions.

Increasing the reduction temperature of the samples to 500 °C resulted in a marked reduction in the H_2 and CO uptakes with H/M and CO/M ratios decreasing to near zero for all samples. Both TiO_2 (P-25) and TiO_2 (Cab-O-Ti) gave the same results. The change in H_2 or CO uptakes with increasing reduction temperature would be expected for all the metals except Pd if extensive agglomeration of the metal component occurred. For Pd the H/M value upon agglomeration is expected to approach, at room temperature, the value of ~0.65

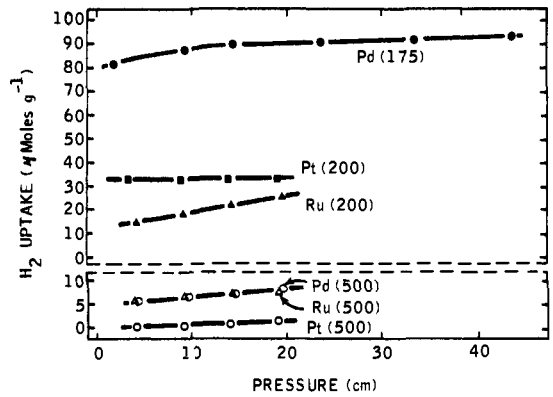

Figure 1. Representative isotherms for H_2 on TiO_2-supported metals. The upper field shows isotherms for low-temperature reductions and the lower field for the high-temperature reductions. The reduction temperature for the respective samples are shown in parentheses.

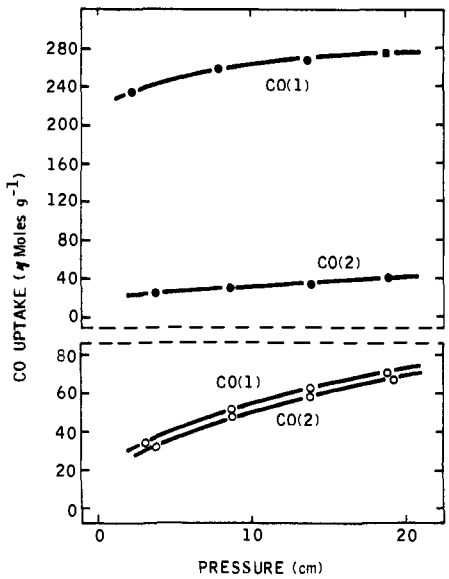

Figure 2. Representative isotherms for CO adsorption on 2% Rh/TiO_2. The upper field shows the CO isotherms following reduction and evacuation at 200 °C. CO(1) is the isotherm on the fresh sample while CO(2) was measured after a 1-min evacuation at room temperature following measurement of CO(1). The lower field shows CO isotherms following reduction at 500 °C.

characteristic of the bulk β-phase hydride.[18] This, however, does not occur. The H/M or CO/M ratios for the other samples reduced at 500 °C would correspond to metal particle sizes ranging from about 10 nm for Os to >25 nm for the other metals. Particles of these sizes should be easily detectable by x-ray diffraction or electron microscopy and these studies were subsequently performed.

X-Ray Diffraction Studies. All samples listed in Table I were examined by x-ray diffraction following H_2 and CO adsorption studies. Figure 3 (A–D) compares three representative samples, all of which had been reduced at 500 °C for 1 h, and a physical mixture of 2% Pd and 98% TiO_2. For none of the samples listed in Table I were sharp x-ray diffraction lines of the metals observable. The 2% Pd/TiO_2 sample gave a pattern which was indistinguishable from that of TiO_2. The 2% Pt/TiO_2 sample showed some intensity in the regions of 2θ where the principal diffraction peaks for Pt are expected. Figure 3-C shows, however, that the lines are very broad and not at all indicative of Pt crystallites >25 nm in size. In order to determine whether metal crystallites of about 10 nm in size could be detected at the 2 wt % loading, a physical mixture of Pd and TiO_2 (2 wt % Pd) was examined. The particle size of the Pd black was determined by x-ray line broadening prior to mixing with TiO_2 to be about 12 nm. As Figure 3-D shows, metal particles of this size at the 2 wt % concentration are easily discerned in the x-ray diffraction pattern. The x-ray studies thus indicate that the low H/M and CO/M values for the metal/TiO_2 samples reduced at 500 °C are not due to metal agglomeration.

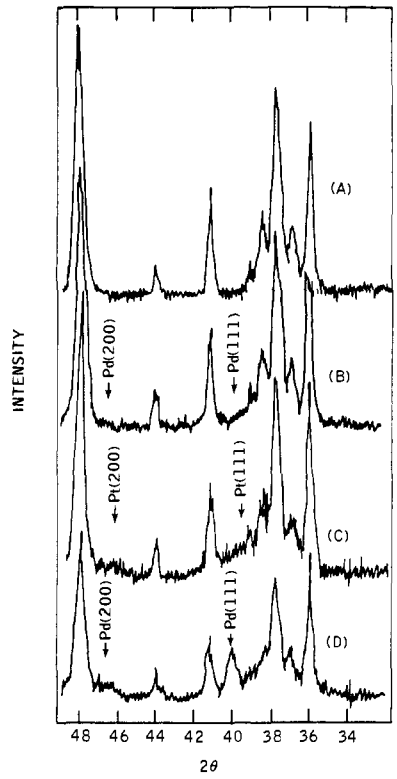

Figure 3. X-ray diffraction patterns for (A) TiO_2, (B) 2% Pd/TiO_2, (C) 2% Pt/TiO_2, and (D) Pd (2%) mixed with TiO_2. All samples except the Pd/TiO_2 mixture were reduced in H_2 at 500 °C for 1 h. Only the ranges of 2θ where the principal diffraction peaks for the metals occur are shown.

Electron Microscopy Studies. Electron microscopic examinations of TiO_2, 2% Pd/TiO_2, 2% Ir/TiO_2, and 2% Pt/TiO_2, all reduced at 500 °C, were carried out at a magnification of 200 000×. At this magnification crystallites >1 nm should be resolved. The micrographs show much variation in contrast owing to differences in the thickness of TiO_2 particles and their overlapping. However, inspection of the transparent areas of the micrographs reveals that the Pt/titanium oxide sample contains many particles in the size range below 5 nm whereas the titanium oxide sample does not. A relatively clear area of the electron micrograph of 2% Pt/TiO_2, in which the metal particles can be discerned, is shown in Figure 4. Copies of the original micrographs may be obtained from the authors. The size distribution for Pt was determined by counting only spherically shaped particles which exhibited higher contrast against the light areas of the support. A total of 175 particles from four micrographs of different areas of the sample were counted. The size distribution obtained is shown in Figure 5. The Pt particles seen by electron microscopy are all less than ~5 nm. We were unable to firmly assess whether the concentration of Pt in the micrographs was representative of the 2 wt % concentration in the sample or whether a significant fraction of the Pt particles was so small as to be unobservable. For the Pt particles counted, the surface diameter, d_{vs}, given by $\Sigma_i f_i d_i^3/\Sigma_i f_i d_i^2$, where f_i is the fraction of particles in the indi-

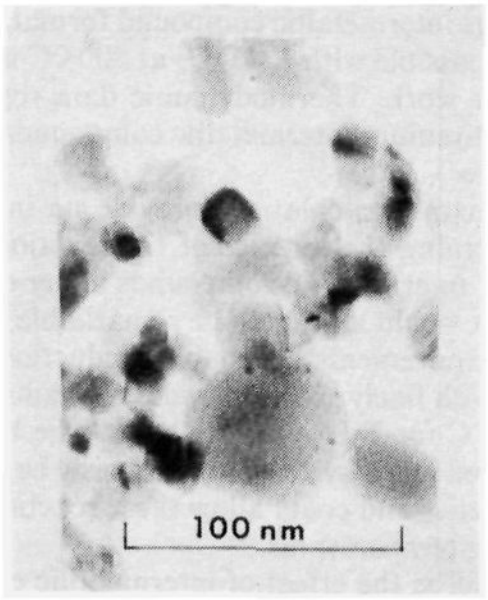

Figure 4. Electron micrograph of 2% Pt/TiO_2 following reduction in hydrogen at 500 °C for 1 h.

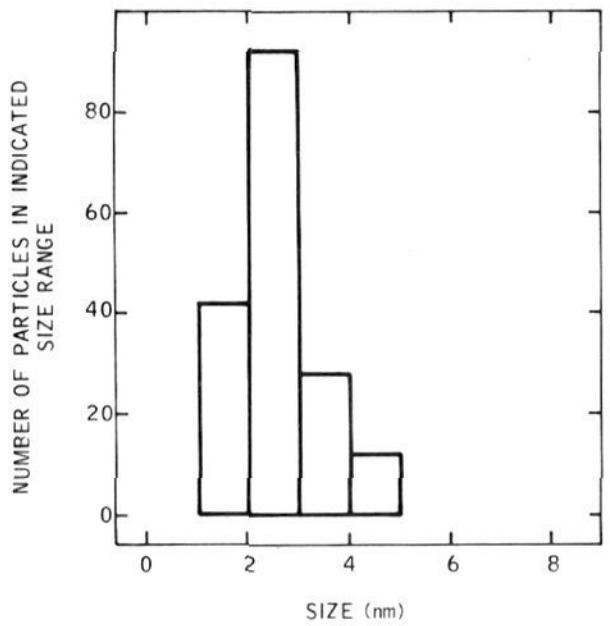

Figure 5. Particle size distribution for 2% Pt/TiO_2 following reduction in hydrogen at 500 °C for 1 h.

cated size range and d_i is the midpoint of the size range, is calculated to be 3 nm. This corresponds to a fraction exposed, $N_{surface}/N_{total}$, of about 0.4 whereas hydrogen and carbon monoxide chemisorption gave values near zero. The microscopy studies thus support the x-ray diffraction results in showing that the Pt crystallites in the Pt/TiO_2 sample are much smaller than are indicated by the H/M or CO/M ratios from the sorption studies.

Analysis of the electron micrographs for 2% Pd/TiO_2 and 2% Ir/TiO_2 gave no evidence for Pd or Ir crystallites greater than ~1 nm whereas the H/M and CO/M ratios were nearly zero. Thus, as was the case for Pt/TiO_2, the H/M and CO/M ratios are not indicative of the Pd or Ir crystallite sizes in these samples.

Effect of Oxidation on Sorption Behavior. Further insight into the nature of the metal/TiO_2 samples was obtained from oxidation studies of Pd/TiO_2. Table III summarizes the results. The effects of hydrogen reduction at 500 °C on the sorption properties of Pd are completely reversible by oxidation. The fresh sample reduced at 175 °C shows a large H/Pd ratio which represents the sum of adsorbed and absorbed hydrogen. Reduction at 500 °C suppresses the sorption of hydrogen and the H/M value of 0.05, even if attributed to adsorbed hydrogen, is inconsistent with the x-ray diffraction and electron microscopy results. Simply rereducing the sample at 175 °C following the 500 °C reduction did not restore hydrogen sorption. Oxidation of the 500 °C reduced sample at 400 °C followed by reduction at 175 °C, however, completely restored the hydrogen sorption capacity relative to the initial treatment. A second reduction at 500 °C again suppressed hydrogen sorption demonstrating the complete reversibility of the effect.

In a separate experiment TiO_2 was treated in H_2 at 700 °C for 2 h followed by air calcination at 600 °C for 4 h. This decreased the BET area of the TiO_2 to 21 $m^2\ g^{-1}$. A 2% Pd/TiO_2 sample was then prepared as described earlier. Following HTR, an H/M ratio of 0.05 was obtained. The suppression of H_2 sorption was, therefore, not dependent on the initial surface area of the TiO_2.

Table III. Effect of Oxidation on Hydrogen Sorption on 2% Pt/TiO_2

Sample	Treatment[a]	H/M
2% Pd/TiO_2	LTR[b]	0.93
	HTR	0.05
	LTR[b]	~0.05
	O_2, 400 °C, 1 h	
	LTR[b]	0.89
	HTR	0.03

[a] Sequential experiments on one sample. [b] Reduction H_2, 175 °C, 1 h, evacuation 1 h, 175 °C.

Discussion

The dihydrogen and carbon monoxide sorption studies show that following low-temperature reduction the noble metals/TiO_2 exhibit expected sorption properties which are indicative of moderate to high metal dispersions. Simply increasing the reduction temperature to 500 °C reduces the sorption of H_2 and CO to near zero but electron microscopy and x-ray diffraction show that metal agglomeration cannot account for the decrease in gas sorption. We shall now consider possible origins of the unique behavior of noble metals supported on TiO_2.

One explanation which must be considered is encapsulation of the metal particles in all the samples following reduction at 500 °C, due to extensive loss of surface area of the support. This would make the metals inaccessible to sorbing gases regardless of particle size. We consider this explanation to be unlikely, however, for the following reasons. Firstly, the BET surface areas of all the samples were essentially the same regardless of whether they were reduced at 200 or 500 °C. Thus no significant loss of support surface area accompanied the reduction at 500 °C. The H_2 and CO sorption properties, however, were markedly affected. Secondly, the effects of reduction at 500 °C on sorption properties were entirely reversible by oxidation of the sample at 400 °C as shown in Table III for Pd/TiO_2. If collapse of the support and encapsulation of the metal were responsible for the loss of H_2 and CO sorption, one would not expect that oxidation could reverse the process. Thirdly, Pd on TiO_2 of 21 $m^2\ g^{-1}$ showed the same H_2 sorption suppression following reduction at 500 °C as did Pd on TiO_2 of 46 m^2/g. The reduction in surface area of the TiO_2 at 700 °C in hydrogen most certainly would have stabilized the support against further surface area loss at 500 °C. The evidence from BET areas, the reversibility of the sorption behavior, and the reduced surface area experiment all argue against encapsulation of the metals to account for the suppression of H_2 and CO sorption on the noble metal/TiO_2 samples.

Poisoning of the metals following reduction at 500 °C is also unlikely to explain the unusual sorption properties of the TiO_2-supported metals. TiO_2 (P-25) contained a number of impurities as shown in Table I. These impurities, however, are common to many supports such as SiO_2 and Al_2O_3 on which expected sorption behavior of noble metals is observed following reduction at 500 °C. If all the sulfur in the TiO_2 (P-25) acted as a poison, it would correspond to only 25 $\mu mol\ g^{-1}$ TiO_2

whereas the Ru, Pd, and Rh on TiO_2 samples contained ~200 μmol metal g^{-1} TiO_2. It is thus unlikely that the small amount of sulfur present could completely poison the metals for H_2 and CO sorption. In addition, oxidation of the sample at elevated temperatures would be expected to remove sulfur adsorbed on the metal and restore "normal" sorption behavior following *reduction at 500 °C.* This was not the case, however, as demonstrated in Table III. Finally, the fact that the high-purity TiO_2 (Cab-O-Ti) gave the same sorption results as the less pure TiO_2 (P-25) argues against impurities being responsible for the suppression of H_2 and CO sorption.

Since encapsulation or poisoning by impurities are unlikely explanations for the unique sorption properties of the noble metal/TiO_2 samples, we must consider the possibility of chemical interactions between the metals and the support. We shall refer to these interactions as strong metal–support interactions (SMSI). In attempting to understand its nature, we are limited by the fact that the evidence for the interaction comes from macroscopic sorption studies of H_2 and CO and it is not clear, at the present time, what chemical perturbations of noble metals would destroy their interaction with H_2 or CO. Nevertheless, we feel that it is useful to consider possible chemical interactions which could occur between noble metals and TiO_2.

It seems plausible that the SMSI effect is associated with the formation of bonds between the noble metal and titanium *cations* or titanium *atoms*, the latter involving the formation of intermetallic compounds. We shall firstly consider the bonding with titanium cations. In the Introduction we referred to metal–metal bonding between titanium cations and noble metal cations as has been described for the hexagonal barium titanates.[9] It was proposed that metal–metal bonding in these compounds resulted from the overlapping of the occupied d orbitals of the noble metal cation with the vacant d orbitals of Ti^{4+}. The hexagonal barium titanates are formed under oxidizing conditions, whereas the interactions observed in our work occur under reducing conditions and the reduced noble metal is the precursor to the SMSI state. It is plausible that the d-electron-rich noble metal could still bond to surface titanium ions in a manner analogous to that occurring in hexagonal barium titanates.

Another kind of interaction between the noble metal and the support which must be considered is the formation of intermetallic compounds. Highly exothermic reactions are known to occur between metals of group 4B (or 5B) and metals of group 8. According to Brewer,[19-21] the driving force in these systems is the donation of electrons from an atom with internally paired d electrons to one with empty d orbitals. There is thus a clear analogy between iridium–titanium bonding in $TiIr_3$ and the Ir^{4+}–Ti^{4+} interaction in $BaIr_{1/3}Ti_{2/3}O_3$.

Meschter and Worrell[22] have investigated the thermodynamics of formation of intermetallic phases in the platinum–titanium system, using a galvanic cell technique operating at 1150–1400 °C. The standard free energy of formation of $TiPt_3$ at 500 °C is calculated from their results to be −75.5 kcal/mol. This can be used to calculate $\delta G°$ for the coupled reduction of TiO_2 in the presence of platinum, i.e.,

$$TiO_2 + 2H_2 + 3Pt \rightarrow TiPt_3 + 2H_2O$$

using values for the free energies of formation of TiO_2 and H_2O obtained from Reed's monograph.[23] The standard free energy change for the coupled reduction is computed to be +18.6 kcal/mol TiO_2 at 500 °C indicating that the formation of $TiPt_3$ will be thermodynamically favored at 500 °C for $(p_{H_2O}p_{H_2}^{-1})$ values $<10^{-2.6}$, i.e., 2500 ppm H_2O in a stream of H_2. Measurements of the H_2O concentration in the exit gas during hydrogen reduction of the noble metal/TiO_2 samples was ~120 ppm at the beginning of HTR but decreased to ~8 ppm after 1 h. Thus intermetallic compound formation is thermodynamically possible with Pt/TiO_2 at 500 °C under the conditions of our work. Thermodynamic data regarding other noble metal–titanium intermetallic compounds are not presently available.

Thermodynamic calculations provide no information, of course, concerning the kinetics of the reaction. The actual occurrence of intermetallic compounds under our conditions of experiment would appear to be remarkable in view of the ultrasevere requirements for coupled reduction reported for experiments with finely ground powder reactants (1200 °C for $TiPt_3$, 1600 °C for $TiIr_3$ and $TiRh_3$).[24] The high degree of metal dispersion in our systems will obviously be favorable with regard to kinetics and could allow these reactions to proceed at much lower temperatures.

What would be the effect of intermetallic compound formation on H_2 and CO sorption? Unfortunately, no information on H_2 and CO sorption on noble metal–titanium compounds is available in the literature. Titanium and intermetallic compounds of Ti with Fe, Co, Ni, and Cu are known to form hydrides.[25] It seems reasonable that hydride formation would also occur with the noble metal–titanium intermetallics and that H_2 adsorption would take place on the surfaces of such compounds. Firm conclusions in this regard, however, must await further experimentation.

What we wish to stress is the possibility of bonding between the noble metal and a titanium entity at the surface—either titanium cations or titanium atoms. It is these unique interactions which give rise to drastic changes in the sorption properties of the metal unlike those possible with conventional supports such as SiO_2 and Al_2O_3. Based on our sorption studies in combination with x-ray diffraction and electron microscopy we feel confident that our data give firm evidence of metal–support interactions of a type not previously recognized. These novel interactions have important implications to heterogeneous catalysis, as well as to solid state chemistry and surface science. A more detailed understanding of the chemical perturbations of the noble metal caused by strong metal–support interactions and the concomitant effect on sorption properties should have implications for theories of chemisorption on noble metals. Further studies of strong metal–support interactions, involving catalytic and sorption properties, as well as instrumental characterization, will be reported in subsequent communications from this laboratory.

Acknowledgments. The authors are indebted to Professor M. Boudart, Department of Chemical Engineering, Stanford University for many helpful discussions during the course of this research and the preparation of this paper. We also acknowledge Dr. E. B. Prestridge, Exxon Research and Engineering Co., Analytical and Information Division, for performing the electron microscopy examinations; Dr. R. T. K. Baker and Mr. R. D. Sherwood of our laboratories for assistance in interpreting the electron micrographs; and Mrs. L. W. Turaew and Miss E. P. Marucchi of our laboratories for skillful execution of the catalyst preparations and chemisorption experiments.

References and Notes

(1) G. Dalmai-Imelik, C. Leclercq, and A. Maubert-Muguet, *J. Solid State Chem.*, **16**, 129 (1976).
(2) R. A. Dalla Betta and M. Boudart, *Proc. Int. Congr. Catal., 5th, 1972*, **2**, 1329 (1973).
(3) P. Gallezot, J. Datka, J. Massardier, M. Primet, and B. Imelik, *Proc. Int. Congr. Catal., 6th, 1976*, **No. A11** (1976).
(4) P. Gallezot, A. Alarcon-Diaz, J. A. Dalmon, A. J. Renouprez, and B. Imelik, *J. Catal.*, **39**, 334 (1975).
(5) A. Magneli and G. Anderson, *Acta Chem. Scand.*, **9**, 1378 (1953).
(6) W. H. McCarroll, L. Katz, and R. Ward, *J. Am. Chem. Soc.*, **79**, 5410 (1957).
(7) P. C. Donohue, L. Katz, and R. Ward, *Inorg. Chem.*, **4**, 306 (1965).
(8) J. J. Lander, *Acta Crystallogr.*, **4**, 148 (1951).

(9) J. G. Dickinson, L. Katz, and R. Ward, *J. Am. Chem. Soc.*, **83**, 3026 (1961).
(10) J. E. Benson and M. Boudart, *J. Catal.*, **4**, 704 (1965).
(11) G. R. Wilson and W. K. Hall, *J. Catal.*, **17**, 190 (1970).
(12) D. J. C. Yates and J. H. Sinfelt, *J. Catal.*, **8**, 348 (1967).
(13) H. P. Klug and L. E. Alexander in "X-Ray Diffraction Procedures for Polycrystalline and Amorphous Materials", 2nd ed, Wiley, New York, N.Y., 1974, p 687.
(14) E. B. Prestridge and D. J. C. Yates, *Nature (London)*, **234**, 345 (1971).
(15) S. Engels, R. Malsh, and M. Wilde, *Z. Chem.*, **16**, 416 (1976).
(16) M. Kobayashi and J. Shirasaki, *J. Catal.*, **28**, 289 (1973); **32**, 254 (1974).
(17) C. R. Guerra and J. H. Schulman, *Surf. Sci.*, **7**, 229 (1967).
(18) M. Boudart and H. S. Hwang, *J. Catal.*, **39**, 44 (1975).
(19) L. Brewer, *Acta Metall.*, **15**, 553 (1967).
(20) L. Brewer, *Science*, **161**, 115 (1968).
(21) L. Brewer and P. R. Wengert, *Metall. Trans.*, **4**, 83 (1973).
(22) P. J. Meschter and W. L. Worrell, *Metall. Trans.*, **7A**, 299 (1976).
(23) T. B. Reed, "Free Energy of Formation of Binary Compounds", MIT Press, 1971.
(24) H. Schulz, K. Ritapal, W. Bronger, and W. Klemm, *Z. Anorg. Allg. Chem.*, **357**, 299 (1968).
(25) K. Yamanaka, H. Saito, and M. Someno, *Nippon Kagaki Kaishi*, **8**, 1267 (1975).

The Hexasilver Molecule Stabilized by Coordination to Six Silver Ions. The Structure of $(Ag^+)_6(Ag_6)$. The Crystal Structure of an Ethylene Sorption Complex of Partially Decomposed Fully Ag^+-Exchanged Zeolite A

Yang Kim and Karl Seff*

Contribution from the Chemistry Department, University of Hawaii, Honolulu, Hawaii 96822. *Received May 2, 1977*

Abstract: The crystal structure of an ethylene sorption complex of partially decomposed fully Ag^+-exchanged zeolite A has been determined from three-dimensional x-ray diffraction data gathered by counter methods. The structure was solved and refined in the cubic space group $Pm3m$; $a = 12.212$ (1) Å at 23 (1) °C. The complex was prepared by dehydration and partial decomposition at 400 °C and 5×10^{-6} Torr for 4 days, followed by exposure to 120 Torr of ethylene gas at 23 °C. Two types of unit cells can be distinguished. About 46% contain, in the sodalite unit, the octahedral molecule Ag_6 complexed to six Ag^+ cations at 6-ring sites to give $(Ag^+)_6(Ag_6)$. The Ag–Ag bond length, 2.850 (4) Å, is notably less than the 2.928 (4) Å distance found in $(Ag^+)_8(Ag_6)$, presumably because fewer cations can draw bonding electron density from the Ag_6 molecule. The Ag–Ag^+ coordination approach is 3.26 (2) Å, less than the distance of 3.33 (1) Å in $(Ag^+)_8(Ag_6)$, presumably because the Ag^+–Ag interaction is correspondingly stronger. The remaining 54% of the unit cells have the following arrangement: one 6-ring Ag^+ ion is in the sodalite unit, and seven others are recessed approximately 1.2 Å into the large zeolite cavity where each forms a lateral π complex with an ethylene molecule. These latter Ag^+ ions are in a near tetrahedral environment, 2.49 (1) Å from three framework oxide ions and 2.54 (8) Å from each carbon atom of an ethylene molecule (which is here counted as a monodentate ligand.) Approximately two additional Ag^+ cations are associated with 8-oxygen rings in all unit cells. Full-matrix least-squares refinement converged to a weighted R_2 index (on F) of 0.071 using the 408 independent reflections for which $I > 3\sigma(I)$.

Introduction

Vacuum-dehydrated fully Ag^+-exchanged zeolite A probably contains uncharged octahedral silver clusters, Ag_6, at the centers of most of its sodalite cavities.[1,2] (With far less likelihood, the clusters could be Ag_5 or Ag_4, whose structures would be octahedra with one or any two vertices, respectively, missing.[1]) These six-atom molecules are closest packed, are the smallest possible fully developed single crystals of silver, and have the natural growth form [111] of silver metal. The number of silver clusters has been observed to increase with dehydration time and temperature until approximately two-thirds of the sodalite units contain silver clusters; the remaining one-third do not. To date, attempts to carry this reaction further have led to the migration of silver atoms out of the zeolite structure, to form crystallites of metallic silver on the surface of the zeolite crystal.[3]

Ammonia gas at 25 °C can also displace the Ag_6 molecules from the zeolite structure. Crystallographic studies[4] have shown that under certain conditions, sorbed ammonia has trimerized and complexed with Ag^+ ions to form the saturated hydronitrogen complexes $Ag_2(N_3H_5)_3^{2+}$ and $Ag(N_3H_3)^+$ within the zeolite, displacing Ag_6 as ligands to Ag^+. At temperatures between 23 and 75 °C, N_3H_3 (cyclotriazane) and N_3H_5 (triazane) have been identified mass spectrometrically in the gas phase above the zeolite.[4]

As a continuation of the study of the unusual chemistry of silver ions, silver clusters, and molecules within this zeolite, an ethylene sorption complex of fully dehydrated Ag_{12}-A[5] was prepared and its crystal structure determined.

Carter et al.[6] have studied the sorption of ethylene at room temperature onto a series of ion-exchanged synthetic near-faujasites by infrared spectroscopy and by microcalorimetry. They found that C_2H_4 molecules form laterally held π complexes of symmetry C_2. Of the transition metal ions examined, Ag^+ and Cd^{2+} were found to hold C_2H_4 most strongly. Furthermore, the adsorbed ethylene molecule is reported to be freely rotating in all cases, except in its Ag^+ complex.

In the crystal structure of an ethylene sorption complex[7] of partially Co(II)-exchanged zeolite A, Co_4Na_4-A, the four Co(II) ions are found at 6-ring[2] sites. Each Co(II) is recessed 0.58 Å into the large cavity where it complexes laterally to an ethylene molecule. The relatively long (2.51 (6) Å) and weak Co(II)–C_2H_4 interaction is ascribed largely to the polarization of the π electron density of ethylene by the highly charged Co(II) ion.

0002-7863/78/1500-0175$01.00/0